STUDIES ON SYNTHESIS AND CHARACTERIZATION OF ZINC OXIDE NANOPARTICLES USING MENTHA ARVENSIS L. LEAF EXTRACT

M. KEERTHANA[1], R. NISHA[1,*]

[1] *Post Graduate and Research Department of Physics Kamban College of Arts and Science For Women, Thenmathur, Tiruvannamalai-606 603 (Affiliated to Thiruvalluvar University, Vellore), Tamilnadu, India.*

ABSTRACT

The synthesized zinc oxide nanoparticles were extensively studied by X-Ray Diffraction (XRD), Fourier Transform Infrared (FT-IR), Field Emission Scanning Electron Microscopy (FE-SEM), and Energy Dispersive X-Ray Spectroscopy (EDX), UV-visible (UV-Vis) and Photoluminescence (PL) analysis.

Keywords: XRD; FT-IR; UV and SEM.

5.1. INTRODUCTION

Nanotechnology is one of the technological innovations in 21st century. Nanotechnology is emerging as a rapidly growing field with its application in science and technology for the purpose of manufacturing new materials at the nano scale level. Nanotechnology can be useful in diagnostic techniques, drug delivery, sunscreens, antimicrobial bandages, disinfectant, a friendly manufacturing process that reduces waste products (ultimately leading to atomically precise molecular manufacturing with zero waste), as catalyst for greater efficiency in current manufacturing process by minimizing or eliminating the use of toxic materials, to reduce pollution (e.g. Water and air filters) and an alternative energy production (e.g. Solar cell and fuel cells) (Meruvu et al., 2011).

The techniques for obtaining nanoparticles using naturally occurring reagents such as vitamins, sugars, plant extracts, biodegradable polymers and microorganisms as reductants and capping agents could be considered attractive for nanotechnology. The fields of synthesis of nanoparticles and assembly have turned to biosynthesis methods for nanoparticle production, which employ plants, fungi, bacteria and enzymes and represent possible ecofriendly alternatives to chemical and physical methods (Nagajyothi et al., 2014). These syntheses have led to the fabrication of limited number of inorganic nanoparticles (mainly metal nanoparticles, although several metal oxides and salts are also reported).

Microorganisms can also be utilized to produce nanoparticles but the rate of synthesis is slow and only limited number of sizes and shapes are amenable compared to routes involving plant based materials. Among the reagents mentioned above, plant based materials seem to be the best candidates and they are suitable for large- scale 'biosynthesis' of nanoparticles. Plant parts such as leaf, root, latex, seed and stem are being used for metal and metal oxide nanoparticle synthesis.

The use of plant extract has advantages such as easy availability, safe to handle and possess a

broad viability of metabolites. Plant extract has been used as reducing and capping agent for the synthesis of nanoparticles which could be advantageous over photochemical reduction, heat evaporation, electrochemical reduction, and chemical reduction methods (Hiremath et al., 2013). Green synthesis of nanoparticles provides advancement over other methods as it is simple, cost-effective and relatively reproducible, more stable materials and eliminate the need of using harsh or toxic chemicals (Kharissova et al., 2013).

2. EXPERIMENTAL PROCEDURE

2.1. Materials

Fresh leaves of Mentha arvensis L. free from disease were collected early in the morning from Thillainayagapuram (North), Chidambaram, Cuddalore District, Tamil Nadu, India. The leaves were identified and authenticated by Department of Botany, Annamalai University. Chemical (Zn (NO3)2.6H2O) and glassware were procured from Sigma Aldrich, Pondicherry, India.

2.2. Synthesis of zinc oxide nanoparticles using Mentha arvensis leaf extract

The amassed Mentha arvensis leaves had been washed with tap water and after that adopted with distilled water for removing the unwanted impurities similar to scum, dirt and other materials. The leaves pattern was allowed to dry in room temperature (32oC) and 40 g was taken for synthesis intent. The weighed of 40 g leaves were boiled with 200 mL of double distilled water for 40 min at 60oC. Mild yellow colored solution used to be formed and it was once cooled at room temperature. The yellow colored extract was filtered with filter paper (Whatman No.1) and stored in refrigerator. In a typical synthesis, the different volumes (10, 20 and 30 ml) of Mentha arvensis, aqueous extract were taken from the stock solution (stored at refrigerator). Later 2 g of zinc nitrate hexahydrate crystal was dissolved in different volumes of (10, 20 and 30 ml) Mentha arvensis extract solution under constant stirring using magnetic stirrer. After complete dissolution of the mixture, the solution was boiled at 60-80°C by using magnetic stirrer until the formation of deep yellow colored paste. The paste was transferred to a ceramic crucible cup and heated in furnace at 400°C for 2 hr. The obtained light yellow colored powder was used for the further studies.

3. Results and discussion

3.1. Structural analysis

The ZnO NPs were prepared from various volumes (20, 30 & 40 ml) of Mentha arvensis leaf extract with fixed zinc nitrate precursor (2 g). The XRD patterns show the noticeable peaks of ZnO at 31.73, 34.43, 36.21, 47.55, 56.56, 62.82 and 67.92° corresponding to (100), (002), (101), 102, (110), (103) and (112) planes respectively as shown in Fig.1. The plane values of XRD patterns are in good agreement with JCPDS No: 89–7102 (Rajiv et al., 2013; Sangeetha and Kumaraguru, 2013). All recorded peaks intensity profiles were characteristics of the hexagonal wurtzite structure of ZnO. There is no remarkable diffraction peaks and other crystalline impurities are not observed. The relatively high intensity of the (101) peak is indicative of anisotropic growth and implies a preferred orientation of the crystallites. The stiff and narrow diffraction peaks were observed for ZnO which indicates that the product has bulk size and also well crystalline structure. In the case of green synthesized ZnO exhibited a gradual decrease in the peak heights with concomitant increase volumes of leaf extract, further supporting the increasing the values of FWHM.

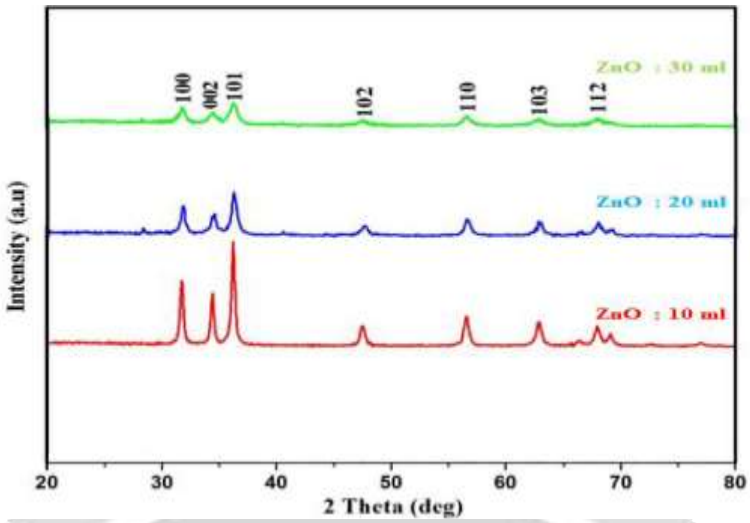

Fig. 1 XRD patterns of the green synthesized ZnO with various volume of Mentha arvensis leaf extract.

Moreover, green synthesized ZnO diffraction peaks were blue shifted when compared to Bare ZnO. The blue shift indicates that the decrease of particles size to increasing volumes of leaf extract. The sizes of the particles were calculated using Scherrer's formula. The size of the particle was calculated using this equation listed in Table 1 The XRD results can be verified by considering the fact that at higher volume of leaf extract the particle surface can effectively be capped to prevent the particle growth, resulting in smaller ZnO NPs. Additionally, the crystal defect parameters like micro strain, dislocation density and lattice constant are calculated using following formula and values are listed in Table 4.1. As in Table 1 the values of micro strain (ε) and dislocation density increase with increasing the volumes of leaf extract due to the presence of active OH functional groups that may inhibit the formation of ZnO in specific shape of lattice.

Table 4.1: Variation of crystallite size, dislocation density, strain and lattice parameters (a and c) for green synthesized ZnO NPs.

Name of the samples	Particles size $Dx10^{-9}$ m	Strain $(\varepsilon)x10^{-3}$	Dislocation density (δ) $x10^{14}$	Lattice parameters (Å) a= 3.249 c= 5.206	
				a	c
ZnO: 10ml	25.32	1.368	15.59	3.259	5.207
ZnO: 20ml	17.41	1.990	32.97	3.249	5.164
ZnO: 30ml	9.23	3.750	117.21	3.252	5.181

The result indicates high number of defects on the surface of smaller size ZnO NPs due to the high surface to volume ratio. The defect related ZnO is more appropriate in photocatalytic and antimicrobial activity. The lattice constants were calculated from (1 0 1) diffraction patterns for bare ZnO and green synthesized ZnO NPs. The values are in close agreement with the literature reports (a = 3.249 A˚; c = 5.206 A˚ Joint Committee on Powder Diffraction Standards file No. 89-7102) with slight deviation.

3..2. FUNCTIONAL ANALYSIS

FT-IR measurement was carried out in the wave number range from 400 to 4000 cm−1 using the KBr

method at room temperature. The FT-IR spectra of Mentha arvensis leaf extract and green synthesized ZnO Fig.2. The FT–IR spectrum of Mentha arvensis confirms the structure of functional with the absorption band at 3344, 2922, 1647, 1415, 1060 829 and 594 cm–1as shown in Table 2.

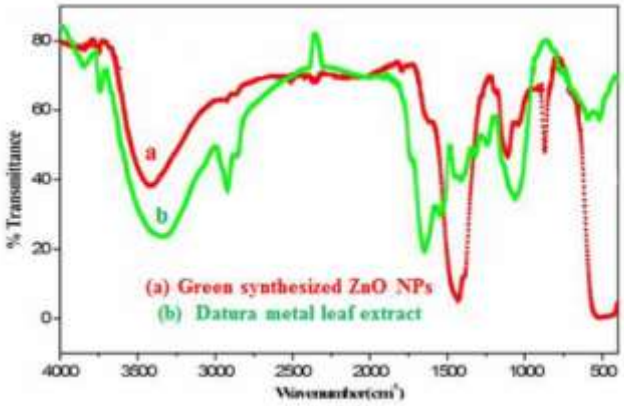

Fig. 2 (a-b) FTIR Spectra of green synthesized ZnO nanoparticles and Mentha arvensis leaf extract.

Table 2 Wave number, stretching and functional groups of leaf extract, green synthesized ZnO.

Wave number (cm^{-1})		Stretching	Functional Groups
Leaf extract	Green ZnO NPs		
3344	3419	O-	Alcohols, Phenols
2922	2926	C-	Alkanes
1647	1616	C=C,N-H	Iºamines
1415	1429	C-C,O-H	Aromatics
1319	1390	C=O,C-H	Alkanes
1244	1192,1111	C-O	Alcohol, Carboxylic Acids, Ester, Ethers
1060	1043	C-	Aliphatic Amines
829	873	C	Aromatics
594	522,424	M	Zn-O

These bands occurred due the enriched photochemical present in the leaf extract such as amino acids, alkaloids, flavonoids and phenolics (Moyo et al., 2012). From FT-IR spectrum of green synthesized ZnO the bands appeared in the lower energy region at 522- 424 cm−1 showing the ZnO bond bending vibration. The region between (600-400) cm–1 is attributed to metal-oxygen (Kundu et al., 2014; Selvarajan and Mohanasrinivasan, 2013; Vimala et al., 2014). The broad band in higher energy at 3419 cm–1 is due to the stretching vibration of the O−H group. The C−H stretching vibration band arises at 2926 cm−1 and depicts the presence of an alkanes group. The band around 1647 cm−1 is due to the amide I and amide II regions that are characteristic of proteins/enzymes. The intense bands observed at (1111-1043) cm−1 C-O and C-N stretching vibration depicts the presence of alcohol, carboxylic acids, ester, and ethers groups. The weaker band located at 873 cm-1 is indicating the presence of C–H (aromatics) group compounds. The overall observation from the Table 2 intensity of peaks are relatively significant

and also proves the existence of some phenolic compounds, terpenoids or proteins that are bound to the surface of ZnO NPs.

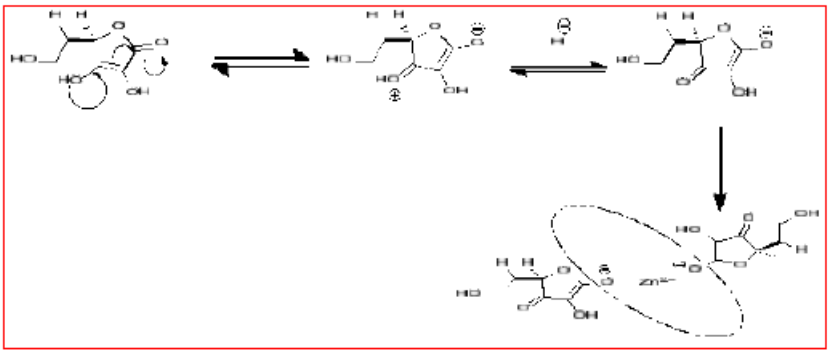

Fig.3 The mechanism of ZnO NPs stabilization from ascorbic acids of Mentha arvensis leaf extract

Changes observed in FTIR spectrum of green synthesis ZnO NPs after bioreduction indicated the participation of polyols, terpenoids and proteins having functional groups of amines, alcohols, ketones, and carboxylic acid in bioreduction reactions. Terpenoids are poorly water-soluble and hence may not be among prime moieties involved in the bioreduction reaction.However, proteins seemed to exhibit little importance in biosynthesis of nanoparticles as reported earlier. Therefore, water-soluble p henolic acid and flavonoid compounds are believed to play a major role in bioreduction reaction. The reduction mechanism of tannin with silver nitrate may also involve in the reduction of silver nitrate to silver nanoparticle. The possible mechanism for the green synthesis of ZnO NPs involves reduction of zinc nitrate ions that can form intermediate complexes with phenolic OH groups present in hydrolysable tannins, which subsequently undergo oxidation to quinine forms with consequent reduction of zinc to zinc oxide nanoparticle. The formation of ZnO NPs can be related to the interactions between reducing phenolic acids such as ascorbic, cardiac glycoside, gallic acid and zinc ions. The mechanism of ZnO NPs stabilization from of Mentha arvensis leaf extracts as shown in the Fig 3.

However the possible mechanism is still unclear and needs further investigation. On the other hand the FT-IR spectrum of bare ZnO indicates that the lower intensity few bands when compared to the green synthesized ZnO and leaf extract. These results confirm the surface of Bare ZnO free from phytochemical.

3.3. FESEM WITH EDX ANALYSIS

Later on the ratification of the FT-IR result the sample was further subjected to FE-SEM studies. Fig.4 (a&b) shows the FESEM image of green synthesized ZnO NPs at different magnifications. The image has showed individual ZnO NPs as well as number of aggregates, particles are spherical and granular nanosized in nature. When an excess of leaf extract (30 ml) was used to reduce the aqueous zinc nitrate the bio-molecules acting as capping agents strongly shaped spherical nanoparticles. Consequently the presence of large quantity of leaf extract, causes strong interaction between protective bio-molecules and surfaces of nanoparticles preventing growth of ZnO nanoparticles and leading to size reduction of spherical nanoparticles (confirmed by XRD results).

The EDX analysis was used to confirm the chemical composition of the ZnO NPs. From EDX spectrum the strong and weak peaks are observed from Zn and O atom as shown in from Fig 4 (c). Additionally, the chemical composition in the Tables 3 clearly indicates atomic and weight percentage of Zn and O elements such as 58.75, 41.25, 25.48 and 74.52

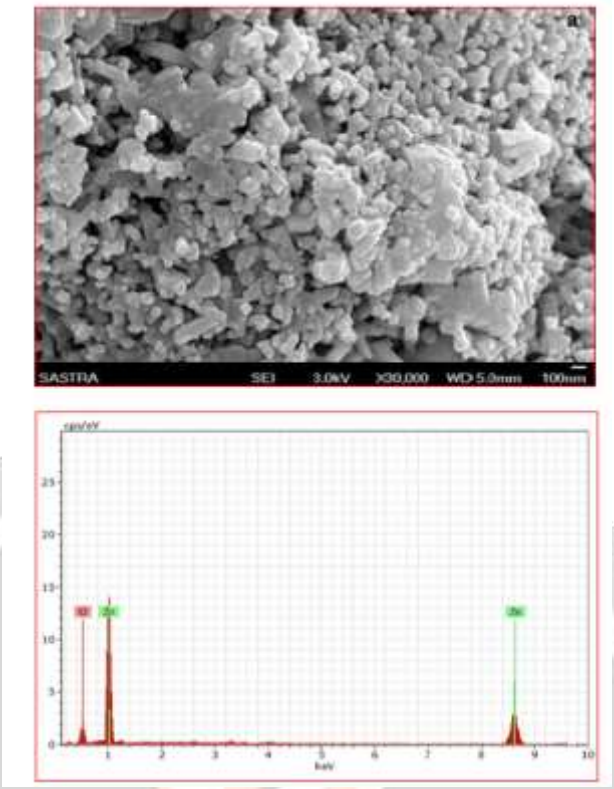

Fig.4 FE-SEM images of different magnification of ZnO nanoparticles (a) X30, 000 (b) EDX spectrum

Tables 3 Chemical composition of green synthesized ZnO

Elements	Atomic number	Series	Weight %	Atomic %
O	8	k-series	25.48	58.75
Zn	30	k-series	74.52	41.25
Total			100.00	100.00

3.4 OPTICAL STUDIES

3.4A. UV-Vis Absorption spectroscopy analysis

The formation of green synthesized ZnO NPs was confirmed by UV– Vis absorption spectroscopic study performed at room temperature with water at 0.1% wt. concentration. The spectrum reveals that the characteristic absorption peak of ZnO at 372 nm (Fig.5a). This peak is originated due to the electron transitions from the valence band to the conduction band (O2p – Zn3d) of ZnO. The band gap energy can be determined by substituting the

value of the absorption peak wavelength using following equation. Applying above equation, band gap energy (Eg) for the green synthesized ZnO nanoparticles was found to be 3.31 eV, The band gap energy can be used to determine the particle size.

3.4B. Photoluminescence spectral analysis

The photoluminescence study is used to investigate the optical properties of as prepared sample. The PL spectrum of ZnO NPs synthesized from the leaf extract of Mentha arvensis is shown in Fig 5 (b). The presence of the peak at 398 nm corresponds to the UV emission in ZnO NPs. The UV emission is attributed to the recombination of free excitons between the conduction and valance bands.

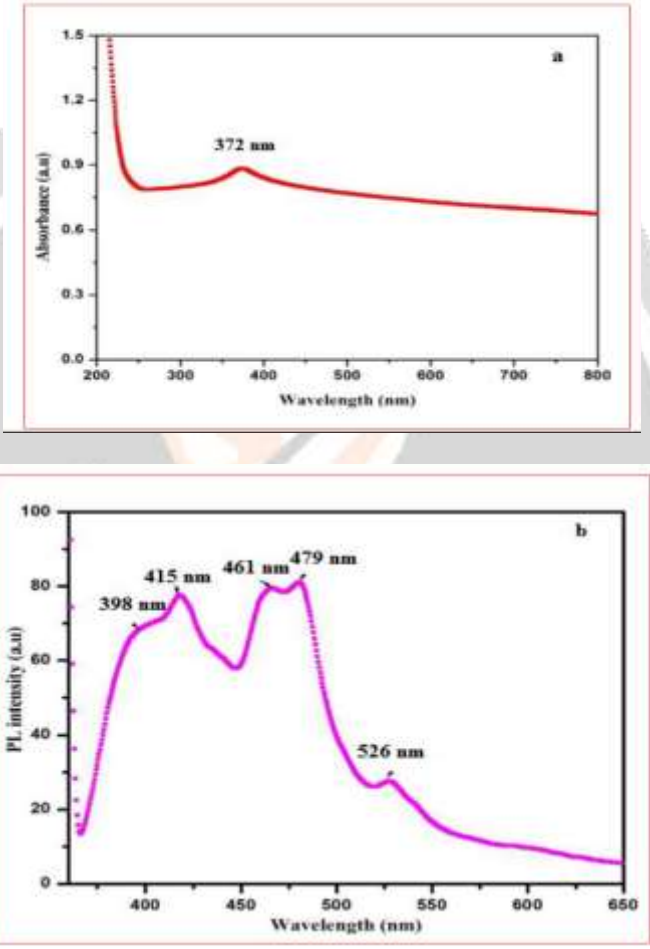

Fig 5 (a&b) UV-vis spectrum and PL spectrum of ZnO nanoparticles synthesized from Mentha arvensis.

The peak observed at 415 nm corresponds to defect related ultraviolet emission. The emission peaks observed at 461 and 479 are assigned to blue emission originates due to transition involving zinc vacancy. Generally, the luminescent region between wavelength 415 nm to 479 nm results due to various defects such as interstitial Zn and the presence of the acceptor and donor states in the region between the valence and conduction bands.

The blue–green emission is assigned to the radiative recombination of photo-generated holes with electrons occupying the oxygen vacancies. The peak observed at 526 nm indicates the presence of green emission originated from the recombination of the hole with the electrons occupying the singly ionized oxygen vacancies. The ZnO NPs show strong, visible emission due to the comportment of a big number of open flaws. This is due to the high surface to volume ratio of ZnO NPs as size decreases; as a result, a large number of defects will be found on the surface.

The PL intensity ratio of the UV band to the blue–green band is proportioned to the defect density in ZnO samples. If higher the PL intensity ratio, the lowers the defect density in the sample.

3. CONCLUSION

The ZnO NPs were prepared from various volumes of Mentha arvensis leaf extract (10, 20 and to 30 ml) with fixed zinc nitrate crystals (2g). The XRD patterns of the ZnO NPs exhibited a gradual decrease in the peak heights with concomitant increase in the width of the peaks further supporting the gradual decrease of particle size (25-9 nm). The FT-IR spectra observed peak in the lower energy region at 522 - 424 cm−1 assigned to the ZnO bond bending vibration.The FE-SEM images show the individual ZnO NPs as well as number of aggregates and particles are spherical and granular nanosized in nature. The size measured and correlated well with the XRD results.In addition, shape of the particles has good agreement with FESEM result. The EDX analysis confirms the chemical composition of the ZnO NPs (Strong peaks and weak peaks are observed from Zn and O atom). The band gap energy (Eg) for the green synthesized ZnO nanoparticles was found to be 3.31 eV. The band gap energy can be used to determine the particle size. In green synthesis process leaf extract acts as capping agent and control the growth of particles size..

REFERENCES

Ahmad, I., Mehood, Z., and Mohanmmad, F., (1998), Screening of some Indian medicinal plants for their antimicrobial properties, J. Ethnopharmacol., 62, 183-193.

Ahmad, I., and Beg, A.Z., (2001), Antimicrobial and phytochemical studies on 45 Indian medicinal plants against multi-dry resistant human pathogens, J. Ethnopharmacol., 74, 113-123.

Amrita Raj and Reena Lawerence, (2018), Green synthesis and charcterization of ZnO nanoparticles from leafs extracts of rosa indica and its antibacterial activity, rasayan j. chem, 11, 1338-1348.

Anbuvannan, M., Ramesh, M., Viruthagiri, G., Shanmugam, N., and Kannadasan, N., (2015), Synthesis, characterization and photocatalytic activity of ZnO nanoparticles prepared by biological method, Spectrochimica Acta Part A, 143, 304–308.

Anbuvannana, M, Ramesh, M, Manikandanc, E, and Srinivasan, R, (2018), Vitex negundo leaf extract mediated synthesis of ZnO nanoplates and its antibacterial and photocatalytic activities, Asian Journal of Nanoscience and Materials, 2(1), 99-110.

Barani, D, Benhaou, B, Laouini, SE, Bentemam, H, Allag, N, Berra, D, and Guerram, A, (2019), Green synthesis of zno nanoparticles using phoenix dactylifera. l leaf extract: effect of zinc acetate concentration on the type of product, digest journal of nanomaterials and biostructures, 14, 581 – 591.

Barzinjy A.A and Azeez H.H., (2020), Green synthesis and characterization of zinc oxide nanoparticles using Eucalyptus globulus Labill. leaf extract and zinc nitrate hexahydrate salt, sn applied sciences, 2,11.

Bhuyan, T., Mishra, K., Khanuja, M., Prasad, R., and Varma, A., (2015), Biosynthesis of zinc oxide nanoparticles from Azadirachta indica for antibacterial and photocatalytic applications,

Bindu P. and Thomas S., (2017), Optical Properties of ZnO Nanoparticles Synthesised from a Polysaccharide and ZnCl2, Acta Physica Polonica A 131.

Chendurpandy, P., Mohan, V.R., and Kalidass, C., (2010), Screening of ethnomedicinal plants for antimicrobial activity. J. Econ. Taxon. Bot., 34, 663-669. Dauthal, P., and Mukhopadhyay, M., (2013), Biosynthesis of palladium nanoparticles using Delonix regia leaf extract and its catalytic activity for nitro-aromatics hydrogenation, Ind. Eng. Chem. Res., 52, 18131-18139.

Chikkanna, MM, Neelagund, S, and Rajashekarappa, K, (2019), Green synthesis of Zinc oxide nanoparticles (ZnO NPs) and their biological activity, sn applied sci., 1, 117.

Chithra, PG, and Vijayalekshmi, V., (2017), Green synthesis, characterization and cyclic voltammetric studies of nano zinc oxide, Int.j. Eng. Sci.Math,, 6, 213-221.

Farfood, ST, Ramazani, A, Moradi, A and Azimzadeh, P, (2019), Green synthesis of zinc oxide nanoparticles using arabic gum and photocatalytic degradation of direct blue 129 dye under visible light, Journal of Materials Science: Materials in Electronics, 28,1-6.

Ghorbani, M, Baharara, J, Eidi, A and Namvar, F, (2019), Green biosynthesis of ZnO nano-particles, inhibited development of pre-antral follicles, Arch. Phar.Practice, 10, 38-49.

Hiremath, S., Vidya, C., Lourdu Antonyraja., M.A, Chandraprabhab, M.N., Gandhia, P., Jaina, A., and Ananda, K., (2013), Biosynthesis of ZnO nano particles assisted by Euphorbia tirucalli (Pencil Cactus), Int. J. Cur. Eng.Technol., 176-79.

Janaki, AC., Sailatha, E., and Gunasekaran, S., (2015), Synthesis, characteristics and antimicrobial activity of ZnO nanoparticles, Spectrochim Acta A, 144 17-22.

Kapadnis Kailas H., Koli Prashant B., Patil Anita P., Jagadale Bapu S., and Hiray Apoorva P, (2016), synthesis of nanocomposites zinc and cobalt ferritepolyaniline by polymerization method, their characterization and bio assay. World Journal of Pharmaceutical Research, 5, 556-563.

Kharissova, O.V., Rasika Dias, H.V., Kharisov, B.I., Pe´rez, B.O., and Pe´rez, V.M.J., (2013), The greener synthesis of nanoparticles, Trends Biotechnol., 31(4), 240-248.

Kundu, D., Hazra, C., Chatterjee, A., Chaudhari, A., and Mishra, S., (2014), Extracellular biosynthesis of zinc oxide nanoparticles using Rhodococcus pyridinivorans NT2: Multifunctional textile finishing, biosafety evaluation and in vitro drug delivery in colon carcinoma, J. Photochem. Photobio. B: Biol., 140,194-204.

Meruvu, H., Vangalapati, M., Chippada, S.C., and Bammidi, S.R., (2011), Synthesis and characterization of zinc oxide nanoparticles and its antimicrobial activity against Bacillus subtilis and Escherichia coli, Rasayan, J.Chem., 4(1), 217-222.

Nagajyothi, P.C., Sreekanth, T.V.M., Tettey, Clement, O., Jun, Y.I., and Mook, S.H., (2014), Characterization, antibacterial, antioxidant, and cytotoxic activities of ZnO nanoparticles using Coptidis Rhizoma, Bioorg. Medi. Chem. Lett., 24, 4298-4303.

Nagajyothi, P.C., Minhan, T.N., Sreekanth, T.V.M., Lee, J.I., Lee, D.J., and Lee, K.D., (2013), Green route biosynthesis:Characterization and catalytic activity of ZnO nanoparticles, Mater. Lett., 108, 160-163.

Narendra Kumar, HK, Chandra Mohana, N, Nuthan, BR, Ramesha, KP, Rakshith, D, Geetha, N and Satish, S, (2019), Phyto-mediated synthesis of zinc oxide nanoparticles using aqueous plant extract of Ocimum americanum and evaluation of its bioactivity, sn applied sciences, 1, 651.

Rajiv, P., Rajeshwari, S., and Venckatesh, R., (2013), Bio-Fabrication of zinc oxide nanoparticles using leaf extract of Parthenium hysterophorus L. and its size-dependent antifungal activity against plant fungal pathogens, Spectrochim. Acta A., 112, 384-387.

Sangeetha, N., and Kumaraguru, A.K., (2013), Extracellular synthesis of zinc oxide nanoparticle using seaweeds of gulf of Mannar, India, J. Nanobiotechnol., 11:39.

Sashikumar, J.M., Remya, M., and Janardhanan, K., (2003), Antibacterial activity of ethnomedicinal plants of Nilgiri Biosphere Reserve and Western Ghats. Asian J. Microbiol. Biotech. Env. Sci., 5, 183-185.

Selvarajan, E., and Mohanasrinivasan, V., (2013), Biosynthesis and characterization of ZnO nanoparticles using Lactobacillus plantarum VITES07, Mater. Lett., 112, 180-182.

Shadmehri, AA, and Namvar, F, (2020), A review on green synthesis method using plant extracts and cytotoxicity and antibacterial mechanisms, J. Res.appl.medi. sci. 6, 23-31.

Varghese, E., and George, M., (2015), Green synthesis of zinc oxide nanoparticles, Int. J. Adv. Res. Sci. Eng., 4 (1), 307-314.

Vidya, C., Hirematha, S., Chandraprabha, M.N, Lourdu Antonyraja, M.A., Venu Gopal, I., Jaina, A., Bansala, K., (2013), Green synthesis of ZnO nanoparticles by Calotropis Gigantea, Int. J.Curr. Eng. Technol., 118-120.

Vimala, K., Sundarraj, S., Paulpandi, M., Vengatesan, S., Kannana, S., (2014), Green synthesized doxorubicin loaded zinc oxide nanoparticles regulates the Bax and Bcl-2 expression in breast and colon carcinoma, Proc. Biochem., 49, 160-172.

Yuhong Zheng, Aiwu Wang, Wen Cai, Bo Deng and Zhi Zhang., (2016), An Electrochemical Sensor Based on Reduced Graphene Oxide and ZnO Nanorods-Modified Glassy Carbon Electrode for Uric Acid Detection, Arabian Journal for Science and Engineering, 41, 135–141.